European Review for Medical and Pharmacological Sciences 2023; 27: 11859-11875

In vitro investigation of the effects of high-intensity therapeutic ultrasound (HITU) in glial tumor cell culture

K.T. OZDEMIR[1], G. AYBERK[2], A. KAZANCI[2], E. SIMSEK[3], C. KABAKCI[4]

[1]Department of Neurosurgery, Medicana International Izmir Hospital, Izmir, Turkey
[2]Department of Neurosurgery, Ankara Yildirim Beyazit University City Hospital, Ankara, Turkey
[3]Department of Cancer Biology, Ankara Yildirim Beyazit University City Hospital, Ankara, Turkey
[4]Global Good Corp., Florida, USA

Abstract. – OBJECTIVE: Amidst the evident challenges posed by brain tumors and the evident limitations of conventional treatment methodologies like surgery, radiotherapy, and chemotherapy, our primary objective was to probe the therapeutic potential of high-intensity therapeutic ultrasound (HITU). The aim was to introduce a safer, cost-effective, and efficient alternative to existing treatments, especially beneficial for inaccessible brain tumor sites and resource-constrained medical facilities.

MATERIALS AND METHODS: Leveraging post-1990s MR technology advancements, we employed the non-invasive HITU technique, akin to high-intensity focused ultrasound. This method directs acoustic energy to tissues, primarily inducing coagulation necrosis by absorbing energy and elevating tissue temperatures. Glial tumor cells were subjected to HITU to assess its effects.

RESULTS: Upon applying HITU to glial tumor cells, significant alterations in cellular structural integrity were evident. The main action of HITU was the absorption of acoustic energy, leading to a notable temperature rise and coagulation necrosis. Flow cytometry indicated significant cellular changes post-HITU. ANOVA and t-test analyses showed a significant relationship between HITU application and time ($p<0.05$). The Shapiro-Wilk test revealed non-normal data distribution ($p<0.05$), leading to the use of non-parametric methods. The t-test results after HITU displayed significant differences ($p<0.05$) in cell counts and fluorescence intensity between control and treated groups. This result was consistent across multiple tests, indicating the reliability of the method in causing cellular damage to the tumor cells.

CONCLUSIONS: Our laboratory analyses offer compelling evidence that HITU is not merely feasible but is also a promising non-invasive approach in the treatment paradigm of brain tumors. Standing distinctively apart from radiotherapy, HITU averts early, or late complications commonly associated with the former. While the path ahead mandates comprehensive research to ascertain its clinical utility, preliminary indications firmly posit HITU as a groundbreaking prospect in the management of brain tumors.

Key Words:
Glioblastoma treatment, Brain tumors, High-intensity focused ultrasound, High-intensity therapeutic ultrasound.

Introduction

Primary central nervous system (CNS) tumors originate from cells located in the CNS, including the sheath or nerves of this structure. Primary CNS tumors consist of a very heterogeneous group, and in the 2016 WHO classification[1], there are 143 different histological subtypes under 17 main titles. The treatments and prognosis of each of these tumors are quite different. Neuroepithelial tumors constitute 30-43.5% of primary CNS tumors[2,3]. Primary CNS tumors are benign or malignant. High-grade neuroepithelial tumors have high morbidity and mortality. Glioblastoma is the most common type of high-grade tumor and constitutes 48.3% of malignant tumors[1]. In a study[4] conducted in Canada, embryonal tumors were the most common type of malignant primary CNS tumor in childhood, and its incidence was reported as $3.36/10^5$/year. Metastatic brain tumors are among the most common secondary malignant tumors of the brain, together with malignant glial tumors[5]. Their prevalence is between 8% and 9.5%, and incidence varies from 8.3 to $14.3/10^5$/year[5].

Corresponding Author: Kaan Tugberk Ozdemir, MD; e-mail: tugberk.ozdemir@medicana.com.tr

Both conventional radiotherapy (RT) and stereotactic radiosurgery (SRS) are an integral part of the treatment of malignant brain tumors today. However, auxiliary treatment methods such as chemotherapy and RT have serious side effects; they are not harmless[6,7]. Radiation toxicity due to RT has serious side effects that occur in the acute, subacute, and late stages[6,7]. The complications that occur, especially in the late period, are called radiation necrosis or radiation myelopathy. Although the incidence of radiation necrosis is not known exactly, it varies between 5% and 50% depending on the dose applied and the follow-up period of the patient[6,7]. In cases of Grade III lesions like anaplastic glial tumors or in some benign tumors such as meningiomas that cannot be operated on due to high surgical risk, serious complications like leukoencephalopathy or radiation necrosis are evident after RT. These complications can also be a concern for patients who are expected to live a long time after treatment and in cases of childhood tumors. It restricts the application of this treatment method in patients up to one year of age and causes complications and a decrease in the quality of life of the patient.

RT and SRS are used especially in the childhood age group when surgery and chemotherapy fail[8]. Many authors[8,9] recommend that RT should be applied after the age of 5 and not applied to patients with neurofibromatosis type 1 (NF1). The relative risk of developing secondary malignancy in patients with NF1 who underwent RT was reported to be 3.04 compared to those with NF1 who did not undergo RT[6].

As RT has serious side effects, can only be applied in limited doses, and cannot be applied to recurrent tumors, it has become necessary to develop alternative treatment methods.

Interest in acoustics, the science of sound, started with Pythagoras's work "Mathematics of Stringed Instruments" in the 6th century BC. Ultrasound is the name given to high frequencies outside the hearing limits of the human ear. The first technological application of ultrasound was developed by Paul Langevin in 1917 for the detection of submarines using ultrasonic methods. Discovered by Jacques and Pierre Curie in 1880, the piezoelectric effect was developed further with the use of transducers developed to generate and detect ultrasonic sound waves. Diagnostic ultrasonography has been used in medicine for about 50 years. It is a very cheap and high-quality alternative to magnetic resonance (MR) and computed tomography among medical diagnostic methods; it is also portable and provides real-time images. Intensified ultrasonography was first used by Lindstrom and Fry[10,11] for tumor ablation purposes in 1954, but technical deficiencies prevented its development. Extracorporeal shock wave lithotripsy (ESWL) was developed in 1980 based on the principle of concentrated ultrasonic waves and received approval from the Food and Drug Administration in 1984[10,11].

High-intensity focused ultrasound (HIFU) does not cause acute, subacute, or late radiation complications, which are among the most common complications of RT-based treatment methods, but it provides effective treatment[12,13]. The basic mechanism of action is that it causes the death of tumor cells as a result of protein denaturation by creating an increase in temperature at the application site[14-16].

It is anticipated that it will be a popular treatment option worldwide in the near future because it is easy to apply and does not have serious side effects. The effect of high acoustic intensity on the tissue and coagulation necrosis due to high temperature because of the absorption of acoustic energy constitutes the main mechanism of action of HIFU.

The main advantages of HIFU are as follows:

- It is a non-invasive method, does not require hospitalization.
- Can be repeated as required.
- Early or late radiation complications such as RT are not seen.
- Low complication and morbidity.
- It can be applied to pediatric patients under appropriate conditions.
- Antitumor, induces an immune response[17].

There are many publications in the literature reporting that HIFU is applied for cancers of various tissues, and its results are beneficial for patients. In 2006, Illing[18] applied HIFU to patients with prostate cancer, and after they published their findings that the tumor had shrunk and no side effects were encountered, it was accepted as a treatment option in Europe[11]. Mottet et al[19] demonstrated in their studies that HIFU could be used in patients with prostate cancer to target cancer cells under MRI guidance without the need for anesthesia or surgical intervention[20]. By controlling the temperature increase in the affected region, tumor cells were destroyed. Their findings[19] were published in 2014 and served as an application guide for the treatment of prostate

cancer. The same team made it a non-invasive treatment method by obtaining approval from the US FDA. It is currently used as a method for treating prostate cancer in some centers in this country. The device named "Sonablate 200" has received the Conformité Européenné (CE) approval for benign prostatic hyperplasia in Europe[18].

As a result of successful research in prostate cancer, studies[21-25] have also been initiated for bone, liver, and lung cancer, bleeding control, and abdominal and gynecological pathologies. Dobrakowski et al[26], who performed research on the brain in the United States in 2014, created an MRI-guided lesion with HIFU in Parkinson's disease. It is currently an FDA-approved treatment for Parkinson's disease. Various studies[17,27] on its use in various movement disorders and psychiatric diseases have also been conducted and are ongoing.

Coluccia et al[28] showed that the tumor shrinks radiologically using HIFU in patients with lung cancer and brain metastasis. Successful results in metastatic brain tumor ablation with subsequent studies led to an increase in research investigating the effect of HIFU on brain tumors. In a study[15] conducted in Zurich in 2014, it was applied to three high-grade brain tumors, and it was reported that it can be applied safely and is beneficial for the patient. In many studies[29], FDA approval was granted on 18.07.2019, depending on the promising results of the use of HIFU in metastatic or malignant brain tumors.

Besides thermal effects, mechanical effects are seen in high-density applications. These include the emergence of additional destructive forces such as cavitation, microcurrent, and radiation forces. The HIFU transducer can apply power of 100-10,000 W/cm^2 to a focal area, and its peak compression pressure reaches 30 MPa with damping pressure up to 10 MPa[10]. Thanks to focusing, a lesion 1 mm in diameter and 9 mm in length is formed[10]. Cavitation depends on compression and expansion of the ultrasonic wave and is diffusive[30]. There are two types: stable and inertial cavitation. Inertial cavitation leads to cell collapse. High-pressure shock waves (20-30,000 bars) and high temperatures (2,000-5,000 K) occur during collapse[11,31]. Micro streaming that occurs during stable cavitation creates temporary defects in the cell wall, and this feature can also be used for intracellular drug delivery[11]. Microstreaming also contributes to tumor shrinkage by causing apoptosis in surrounding cells[11].

In our study, we planned to evaluate the effect of high-intensity therapeutic ultrasound (HITU), which has the same modality as HIFU, on the viability of glioblastoma cells in the laboratory environment at the microscopic and molecular level[32].

Materials and Methods

Cell Preparation and Culturing

Cell source and maintenance

The study employed glioblastoma cell lines from a 60-year-old female patient (ATCC CRL-3412), which were cryogenically stored in a liquid nitrogen tank at -80°C.

Thawing and seeding

The cells were gently thawed in a water bath set at 37°C. After thawing, they were immediately placed into flow cytometry to ensure viability and roughly divided into six equal samples[33]. Each sample was seeded onto six 75-cm² flasks (Nest Scientific 708003) pre-coated with polymeric protein or peptide to enhance cell adhesion[34]. Culture media, as described by Arora's 2017 compilation, was added to facilitate growth[35-37].

Post-thawing, the glioblastoma cells were seeded into polymeric protein or peptide-coated 75-cm² culture flasks and incubated under controlled conditions of 37°C with a CO_2 concentration of 5% to ensure optimal cell growth conditions[38]. The incubation environment was maintained using a state-of-the-art cell culture incubator, ensuring uniform temperature and CO_2 distribution.

Cellular Adhesion and Growth Assessment

After an incubation period of 24 hours, cellular adhesion to the flask surfaces was assessed using a high-resolution phase contrast microscope. Observations revealed that the majority of the cells had adhered well to the surface and showed limited motility, indicating healthy cell attachment. Following this observation, the flasks were returned to the incubator for an extended period of 72 hours to facilitate cell proliferation further.

Subculturing and Group Delineation

Post 72-hour incubation, the flasks were carefully removed, and the cells were examined microscopically to assess their growth and confluency. Utilizing a standardized protocol based on the

methods described by Fedoroff and Richardson[39], the cells were harvested from the flasks, and their counts were ascertained using flow cytometry.

Thereafter, the cells were segregated into three primary groups:

Group 1: Cells were further subdivided and seeded into six 25 cm^2 flasks, ensuring even distribution.

Group 2: This group was further delineated into six subgroups. Each subgroup received approximately 500,000 cells and was then transferred to the incubator to achieve optimal growth conditions.

Group 3: For high-throughput assays, cells were allocated to 96-well plates, with each well receiving approximately 10,000 cells. Six such plates were prepared and placed in the incubator.

Growth Confirmation and Further Procedures

After an incubation duration of 24 hours, the flasks and plates were retrieved, and cellular adhesion was again confirmed using microscopic evaluation. After another incubation period of 72 hours, the cells achieved optimal growth and were deemed ready for subsequent experimental procedures.

HITU Experimental Setup and Equipment Specifications

The High-Intensity Focused Ultrasound (HITU) experiment necessitated an intricate and calibrated setup. Herein, we delineate the assembly process and characteristics of the equipment employed (Figure 1):

Test pool configuration

- The experimental pool was constructed using a transparent acrylic sheet with dimensions of 800 × 800 × 800 mm and a thickness of 10 mm. This was meticulously rendered watertight to ensure accurate HITU applications.
- Stability was of paramount importance. As such, an anchoring frame was fashioned from an 80 × 40 mm Sigma aluminum profile. This frame ensured that the test specimens and measuring sensors remained suspended and stable within the aqueous environment of the test pool.

Flask positioning

- A channel, precisely fitting the dimensions of a tissue flask, was carved into a 100-mm thick acrylic plate. This allowed for the secure placement of the tissue flask while maintaining sterile conditions.

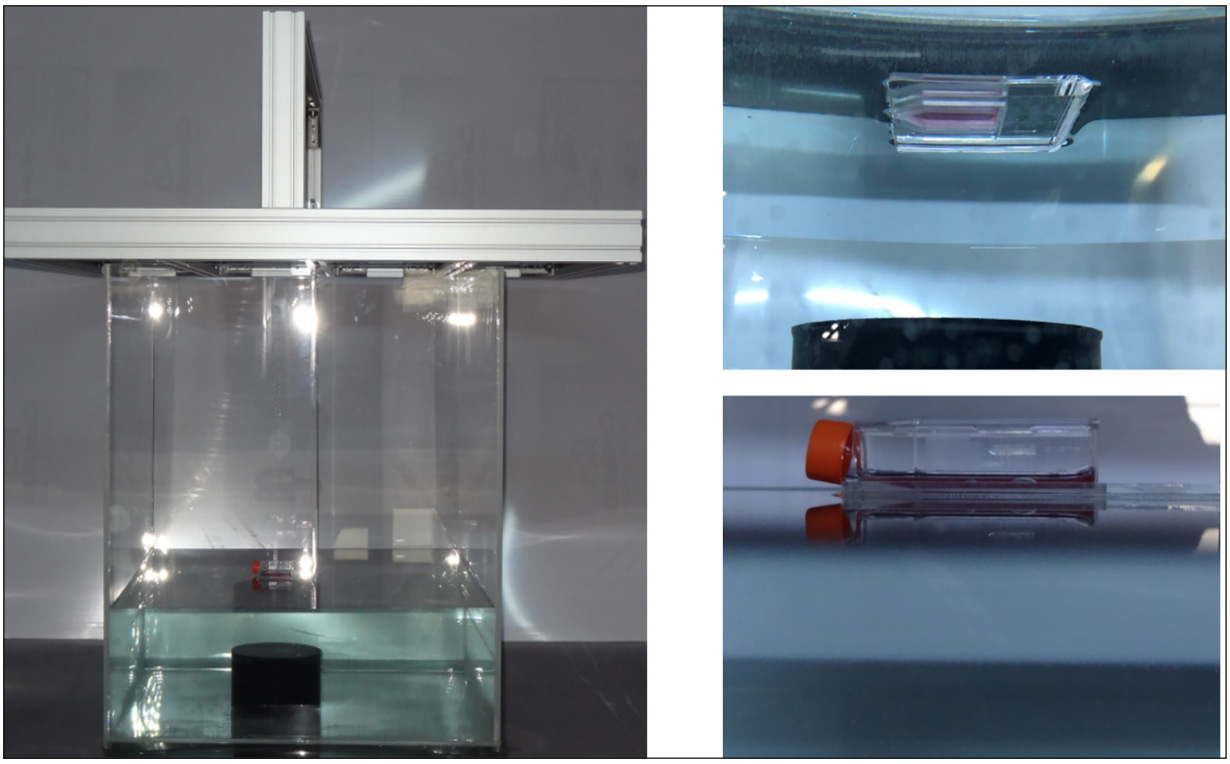

Figure 1. The experimental setup and the flask with glioblastoma cells.

- For precision-focused ultrasound applications, the base of the flask was oriented along the z-axis such that its bottom coincided with the HIFU focal point.

HIFU transducer installation

- The HIFU transducer was positioned on the base of the test pool. An aperture was engineered on the pool's base to accommodate the transducer's cabling.
- Following the transducer's secure affixation, silicone sealant was applied to waterproof the aforementioned aperture, preventing potential water ingress that could compromise the experiment.

Water quality control

- The test pool was filled with meticulously degassed water, maintaining a constant temperature of 36.5°C. Temperature monitoring was facilitated by a calibrated PCE-T 318 thermometer (PCE Instruments, Southampton, Hampshire, United Kingdom).
- To ascertain water quality and purity, the degassed water's conductivity was gauged and recorded as 0.1 μS/cm, using the Hanna Dist 4 Conductivity Meter - HI 98304 (Hanna Instruments, Woonsocket, Rhode Island, USA).

Transducer specifications

- The pivotal component of the HITU setup was the transducer. We utilized a custom-designed HIFU transducer (H-149, Sonic Concepts, Inc., Bothell, WA, USA) characterized by an aperture diameter of 180 mm. It was a single-element, concave piezo composite device with a focal length of 120 mm. Operating at a frequency of 1 MHz, it possessed an electrical power capacity of 1,000 W.

Treatment Protocols

In the quest for non-invasive therapeutic modalities, HITU has emerged as a novel tool. Its efficacy was illustrated when Jacquelyn MacDonell and her team (2018) employed HITU to target a specific brain tumor region[27]. They ablated an area of approximately 2 cm^3 for a duration of 180 seconds, utilizing an acoustic power of 4 W, effectively raising the temperature within the targeted region to achieve therapeutic ablation[27].

Pulse configuration and administration

The flask positioning platform was the focal point for the HITU pulses. Each pulse had a duration of 45 ms, and a total of 50 such pulses were consistently dispatched at intervals of 100 ms. The resultant temperature escalation at the focal point was recorded at 58°C.

Group designations and protocols

Control Groups:

Group 1 comprised three flasks (a1, b1, c1) of 25 cm^2 each, which were kept untreated. Subsequent examinations were carried out under a phase contrast microscope immediately post-incubation, then at 4-6 hours, and finally at 24 hours[40]. Cellular adhesion properties were particularly studied and juxtaposed with established glioblastoma cell line research[40].

Group 2: Encompassed flasks a2, b2, and c2, which also remained untreated. After incubation, cells were prepared for flow cytometry to enable accurate cell counting as they traversed the flow channel[33].

Group 3: Organized as three sets of 96-well plates (a3, b3, c3). Post incubation, ATP activity, and cell viability were gauged using the ATPlite 1Step Luminescence Assay System kit (PerkinElmer, Waltham, MA, USA), strictly adhering to the procedures proposed by Sughrue et al[41].

HITU-treated Groups:

Group 4: Corresponding to Group 1, flasks d1, e1, and f1 underwent HITU treatment. Subsequent microscopic examinations were scheduled identically to Group 1.

Group 5: In alignment with Group 2, flasks d2, e2, and f2 received HITU. Post-treatment, they were destined for flow cytometric evaluations, with timings mirroring Group 2.

Group 6: Analogous to Group 3, these 96-well plate clusters (d3, e3, f3) were treated with HITU. Post-treatment ATP activity and cell viability assessments were conducted in line with Group 3 protocols.

Assessment Techniques

Microscopic Examination: Cells were assessed for morphological changes under a phase-contrast microscope immediately after the respective treatments.

Flow Cytometry: Cellular enumeration was performed using flow cytometry based on the techniques described by Fedoroff and Richardson[39].

ATP Activity and Cell Viability: ATP activity and cell viability were determined using the ATPlite 1Step Luminescence Assay System kit, following the protocol by Sughrue et al[41].

Statistical Analysis

Repeated measures of ANOVA were employed for the assessment of the impact of HITU on cell numbers.

To evaluate the relationship between the HITU application and the elapsed time, a null hypothesis (Ho) was formulated, suggesting no significant connection between the two factors. This hypothesis was tested using the recorded *p*-value.

Further, for all six experimental scenarios, the data's normal distribution was assessed. The Shapiro-Wilk normality test was utilized for this purpose. If the data did not follow a normal distribution ($p<0.05$), nonparametric methods were chosen for the ensuing analysis.

Statistical Analysis

A dependent *t*-test was conducted to assess the statistical significance of differences in cell numbers and fluorescence intensity between the control and application groups, post-high-intensity focused ultrasound (HITU) application. The SPSS (IBM Corp., Armonk, NY, USA) was used for the statistical analysis, and for the findings to be considered statistically significant, the *p*-value had to be lower than or equal to 0.05.

Results

Microscopic Evaluation

For Group 1, which was designated as the control group, the flask was removed from the incubator before the application and immediately (a1) (Figure 2), 4-6 hours later (b1) (Figure 3), and 24 hours later (c1) (Figure 4) and imaged under the phase contrast microscope. Typical glioblastoma phenotypes attached to the flask surface were recorded[40].

In the group determined as Group 4 after HITU was applied, when we looked under the microscope immediately after the application of HITU, which we determined as a1, no visible changes were detected in the cells.

When examining under the microscope 4-6 hours after the application of HITU to the areas designated as e1 and b1, we observed a decrease in the number of cells attached to the surface in the treated part. Additionally, changes were noted in the morphology of both the treated area and the cells in its immediate vicinity (Figure 5).

In our examination using the microscope 24 hours after the HITU application, which we determined as f1, c1, we observed that there were no cells adhering to the surface in the area where we applied HITU, and there was a serious increase in the cells floating in the nutritional fluid. We detected deformities in the shapes of the very few cells attached to the surface, which we can clearly see when compared with normal glioblastoma cell shapes (Figure 6).

Figure 2. Image of our control group (a1) immediately after removal from incubator, 320× magnification.

Figure 3. The next image of our control group (b1) after 4-6 hours, 320× magnification.

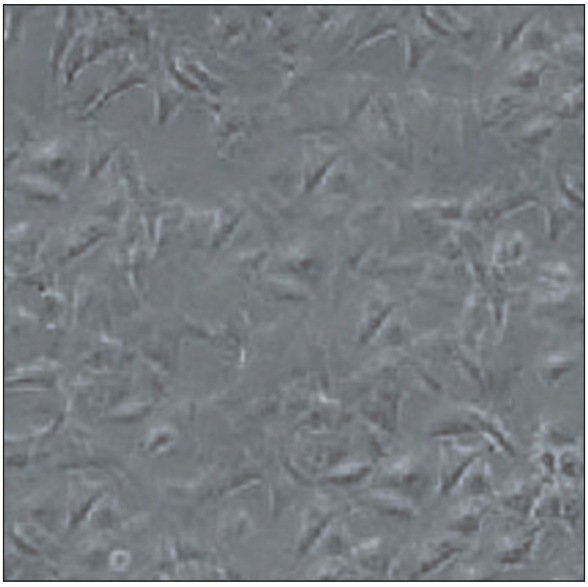

Figure 4. The next image of our control group (c1) after 24 hours, 320× magnification.

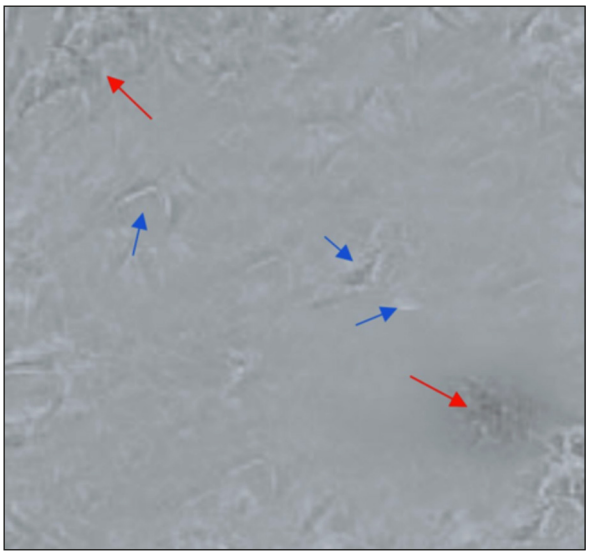

Figure 6. Although we see the cells (*red arrows*) proliferating 24 hours after HITU was applied to our group, which we designated as f1, we see a decrease in the overall cell number and cell remnants (*blue arrows*), 320× magnification.

Flow Cytometer Measurements

We placed approximately equal amounts of initial cells in flasks designated as Group 2 (a2, b2, and c2). After removing them from the incubator, where no action was taken, we observed the cells immediately after applying HITU (labeled as d2), then again after 4-6 hours (e2), and finally at 24 hours. The number of cells in the groups, which we identified as Group 5, were counted using the flow cytometry device following the designated point (f2), and the results are summarized in Table I.

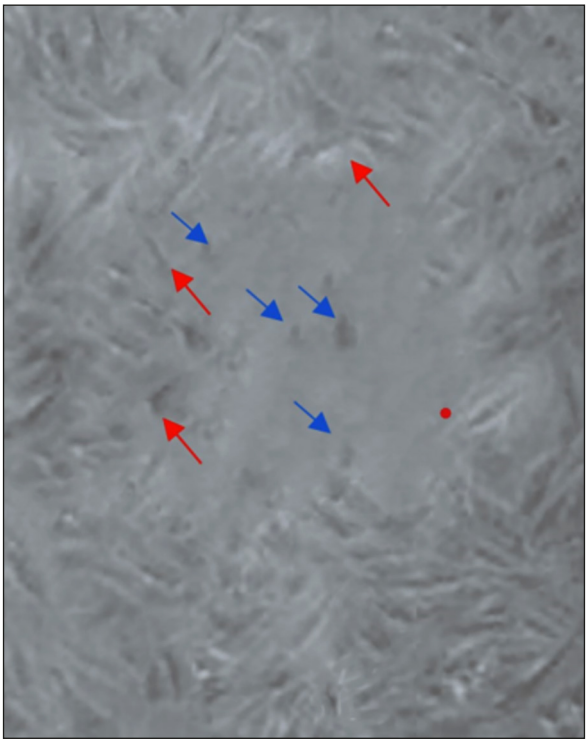

Figure 5. After HITU was applied to our group, which we designated as e1, we see the change in the shape of the cells (*red arrows*) and cell remnants (*blue arrows*) in the sections it was applied to, 320× magnification.

ATP Measurement

We designated the 3rd group (a3, b3, c3) as the control group. Measurements were made immediately after applying HITU to the cell lines (marked as d3), then again after 4-6 hours (e3), and finally after 24 hours (f3). These measurements, which were taken in the groups identified as Group 6, are shown in Figure 7.

Statistical Analysis

The graph of flasks measured by flow cytometry is shown in Figure 8. We utilized repeated ANOVA to examine the effect on the number of cells after HITU application, and the details of this analysis are given in Table II[42].

Whether there is a relationship between HITU application and the time elapsed is shown in Table II.

- The Ho hypothesis is established.
- Ho: There is no significant relationship between the application and the time elapsed.

Table I. Cell numbers after flow cytometry measurement.

	Number of cells put in flasks	Number of cells immediately after incubation/after administration	Number of cells after 4-6 hours	Number of cells after 24 hours
a2 (control)	500,000	500,000	600,000	1,000,000
b2 (control)	500,000	490,000	580,000	980,000
c2 (control)	500,000	500,000	580,000	970,000
d2	500,000	480,000	440,000	550,000
e2	500,000	460,000	390,000	450,000
f2	500,000	490,000	420,000	500,000

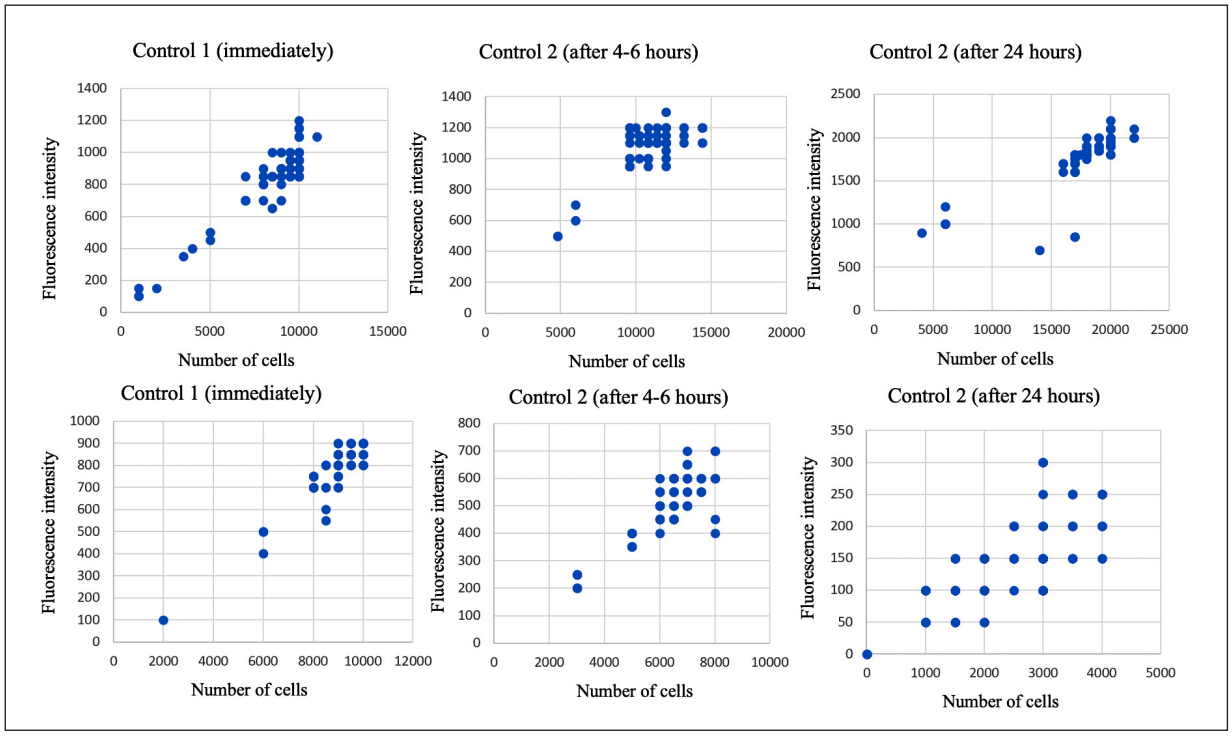

Figure 7. Cell numbers and fluorescence density after ATP kit application.

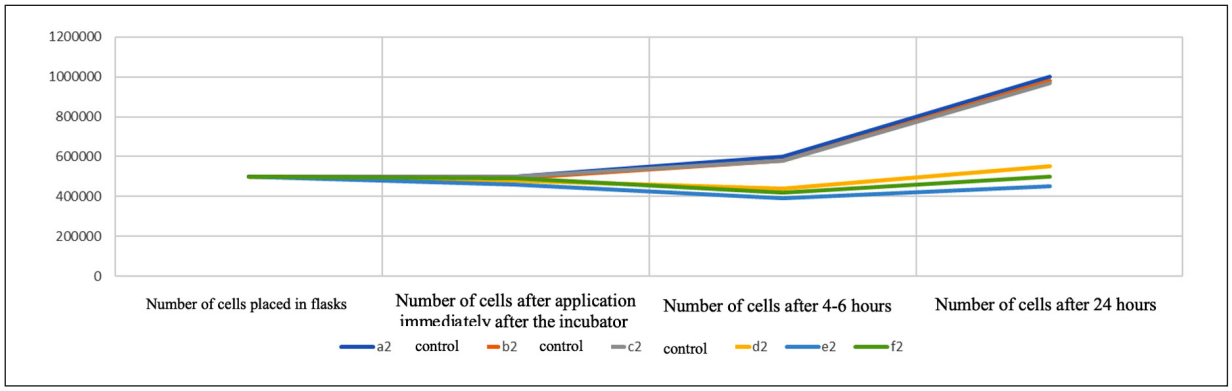

Figure 8. Cell count plot with flow cytometry.

Table II. Examination of cell numbers by repeated ANOVA.

		Number of cells placed in flasks	Immediately after the incubator/number of cells after practice	Cell count after 4-6 hours	Cell count after 24 hours	Total	
Summary							
	Control						
Number		3	3	3	3	12	
Total		1,500,000	1,490,000	1,760,000	2,950,000	7,700,000	
Average		500,000	496,666.7	586,666.7	983,333.3	641,666.7	
Variance		0	33,333,333	1.33E+08	2.33E+08	4.39E+10	
	Practice						
Number		3	3	3	3	12	
Total		1,500,000	1,430,000	1,250,000	1,500,000	5,680,000	
Average		500,000	476,666.7	416,666.7	500,000	473,333.3	
Variance		0	2.33E+08	6.33E+08	2.5E+09	1.88E+09	
	Total						
Number		6	6	6	6		
Total		3,000,000	2,920,000	3,010,000	4,450,000		
Average		500,000	486,666.7	501,666.7	741,666.7		
Variance		0	2.27E+08	8.98E+09	7.12E+10		
ANOVA							
	Source of variance	**SS**	**df**	**MS**	**F**	***p*-value**	**F criterion**
Example		1.7E+11	1	1.7E+11	361.0973	2.1E-12	4.493998
Columns		2.72E+11	3	9.07E+10	192.6726	9.14E-13	3.238872
Interaction		2.24E+11	3	7.48E+10	158.8319	4.08E-12	3.238872
Inside		7.53E+09	16	4.71E+08			
Total		6.74E+11	23				

Since the *p*-value is <0.05, the Ho hypothesis is rejected. There is a significant relationship between the application and the time elapsed.

When we look at the average number of cells in the control group and the treatment groups according to the time elapsed after the application, we see that the average number of cells increased as time passed in the control group after the application. However, we have shown by statistical analysis that the cells in the group to which we applied HITU increased significantly less than those in our control group.

Statistical analyses after the study performed with the ATP measurement kit are shown in Table III.

Since it was tested whether the data were normally distributed for all 6 experimental cases,

- The Shapiro-Wilk normality test was used[43].
- Ho absence hypotheses were established.
- Ho: The data are normally distributed.

When we look at the test results, the Ho hypothesis is rejected because the *p*-value is <0.05. The data are not normally distributed.

- The fact that the data are not normally distributed means that we will use nonparametric methods for analysis.
- The dependent *t*-test is used for our dataset[44].
- There is no significant difference in the cell number measurements taken immediately after the HITU application in the control and application groups, but there is a significant difference in the fluorescence intensity measurements. Here, there is a decrease in the values after the HITU application.
- There is a significant difference in the cell number measurements taken 4-6 hours after the HITU application in the control and administration groups. Cell numbers decreased, and the treatment group showed a notably lower average in fluorescence intensity measurements.
- There is a significant difference in the cell number measurements taken from the control and application groups 24 hours after HITU application. The cell number is about 7 times less than that of the control group. There is a significant difference in fluorescence intensity measurements. The application group's average is lower.

Table III. The relationship between the Shapiro-Wilk normality and dependent *t*-test and the cell number and ATP fluorescence density decrease after HITU.

***t*-test: comparative analysis of averages (shortly after)**			***t*-test: comparative analysis of averages (4-6 hours later)**			***t*-test: two examples of comparative analysis of averages (24 hours later)**		
Cell numbers			**Cell numbers**			**Cell numbers**		
	Control 1	**Practice 1**		**Control 2**	**Practice 2**		**Control 3**	**Practice 3**
Average	8,796.875	8,968.75	Average	11,135.42	6,203.125	Average	17,755.21	2,447.917
Variance	4,255,674	1,356,908	Variance	3,208,838	1,703,043	Variance	11,715,762	1,176,206
Observation	96	96	Observation	96	96	Observation	96	96
Pearson correlation	0.306151		Pearson correlation	0.148412		Pearson correlation	0.497727	
Projected average difference	0		Projected average difference	0		Projected average difference	0	
df	95		df	95		df	95	
t Stat	-0.82753		*t* Stat	23.5305		*t* Stat	49.45593	
p (T≤*t*) single-ended	0.205005>0.05		*p* (T≤*t*) single-ended	1.03E-41<0.05		*p* (T≤*t*) single-ended	6.67E-70<0.05	
t critical single-ended	1.661052		*t* critical single-ended	1.661052		*t* critical single-ended	1.661052	
p (T≤*t*) two-pronged	0.410009		*p* (T≤*t*) two-pronged	2.07E-41		*p* (T≤*t*) two-pronged	1.33E-69	
t critical two-pronged	1.985251		*t* critical two-pronged	1.985251		*t* critical two-pronged	1.985251	
***t*-test: two examples of comparative analysis of averages (shortly after)**			***t*-test: two examples of comparative analysis of averages (4-6 hours later)**			***t*-test: two examples of comparative analysis of averages (24 hours later)**		
Fluorescence intensity			**Fluorescence intensity**			**Fluorescence intensity**		
	Control 1	**Practice 1**		**Control 2**	**Practice 2**		**Control 3**	**Practice 3**
Average	860.4167	794.7917	Average	1,083.854	494.7917	Average	1,780.729	146.875
Variance	44,521.93	15,183.11	Variance	44,521.93	15,183.11	Variance	18,499.73	5,042.763
Observation	96	96	Observation	96	96	Observation	96	96
Pearsoncorrelation	0.419118		Pearson Correlation	0.419118		Pearson Correlation	0.064809	
Projected average difference	0		Projected average difference	0		Projected average difference	0	
df	95		df	95		df	95	
t Stat	3.302336		*t* Stat	3.302336		*t* Stat	32.69177	
p (T≤*t*) single-ended	0.000676<0.05		*p* (T≤*t*) single-ended	0.000676<0.05		*p* (T≤*t*) single-ended	8.76E-54<0.05	
t critical single-ended	1.661052		*t* critical single-ended	1.661052		*t* critical single-ended	1.661052	
p (T≤*t*) two-pronged	0.001352		*p* (T≤*t*) two-pronged	0.001352		*p* (T≤*t*) two-pronged	1.75E-53	
t critical two-pronged	1.985251		*t* critical two-pronged	1.985251		*t* critical two-pronged	1.985251	

Discussion

Due to the advancements in technology and the implementation of minimally invasive procedures, new diagnostic and therapeutic methods have emerged, drastically elevating the quality of life for patients[45,46]. Ostrom et al[47,48] emphasized that such improvements not only lead to decreased morbidity but also curtail treatment expenses. A significant conduit of these progressions has been the translation of advancements in basic sciences to clinical practice, which has been materialized through multidisciplinary studies, as indicated by Weller et al[49]. These integrations have significantly improved patient longevity and comfort.

Addressing the symptoms of a brain tumor is of paramount importance. As highlighted by Sanai and Berger[50], the immediate response should be to manage the presenting symptoms. This involves initiating treatments such as antiedema and, when necessary, antiepileptic interventions, among others. Historically, surgical excision has been recognized as the gold standard for brain tumor management. The principal objectives of such surgical interventions, as described by Stupp et al[51], encompass tissue diagnosis acquisition, mass effect and tumor burden reduction, and enhancement of both lifespan and quality of life.

However, it is essential to note that despite the best efforts in surgical resection, achieving complete excision of malignant glial tumors remains a challenge. Louis et al[52] elaborated on the inherent invasive and infiltrative nature of these tumors, combined with the presence of resilient tumor stem cells, which constrains total eradication. Additionally, the tumor's localization in functional regions often acts as a deterrent for comprehensive excision, as highlighted by Sanai et al[53]. Consequently, post-operative measures such as radiotherapy and chemotherapy, as discussed by Wen and Kesari[54], have become conventional practices for treating high-grade glial tumors.

Presently, pivotal determinants that influence a patient's life expectancy post brain tumor treatment include age, Karnofsky Performance Scale (KPS) scores, tumor dimensions, its location, and the extent of resection performed[55]. In their study, Smith et al[56] and Jones and Brown[57] have similarly highlighted these factors. Comparing our findings with theirs provides a comprehensive understanding of the treatment landscape for brain tumors. The consensus emphasizes individualized patient treatment plans, given the multifaceted nature of influencing factors.

Nowadays, RT stands as a pivotal component in the arsenal of supportive treatments post-surgery, often complemented by chemotherapy. Yet, both therapeutic avenues present their own set of complications. As explored by Patel et al[58], the adverse reactions to RT are broadly classified into acute, subacute, and late phases, with an incidence spanning between 5-50% of the patient cohort. Radiation damages may manifest even at dosages as minimal as 50 Gy, and the combined administration of chemotherapy can elevate these risks[6]. Three dominant mechanisms underscore the etiology of radiation-induced damage:

1) Direct assault on glial/oligodendroglial cells and neural stem cells
2) Impairment of endothelial cells and degradation of the blood-brain barrier
3) Activation of immune-mediated responses[6].

Managing glioblastoma and other brain tumors poses not only medical but also economic challenges. A study by Wang et al[59] underscored that the immediate costs associated with treating brain tumor patients could average around $8,478 monthly. Beyond the tangible expenses, intangible costs manifesting as job losses and early retirements are estimated to contribute approximately 197.7 million dollars, as was the scenario in Sweden[45]. These insights accentuate the pressing need for cost-efficacy analyses to streamline the best therapeutic strategies.

Historically, the inception of ultrasonography as a diagnostic tool can be traced back to the 19th century. Progressive breakthroughs found in the works of Taylor and Green[60] have elucidated the intricate mechanisms of ultrasound waves. This evolution, augmented by technological advancements, has culminated in the emergence of innovative therapeutic interventions. Ultrasound therapy, in particular, is gaining attention as a viable alternative to RT, primarily due to its non-invasiveness and reduced complication index[61].

HIFU technology, pioneered by researchers like Foster and Zhang[62], offers the capability to fine-tune ultrasonic waves, zeroing in on a specific locus, thereby allowing controlled thermal regulation at the targeted site. In MR-guided HIFU, the core principle revolves around sonication – a process wherein a localized region is subjected to ultrasound-induced heating. The

extent of tissue exposure and the duration thereof determine the resultant thermal dose, which, in essence, defines the boundaries of the thermal lesion[11]. Implementing HIFU as a therapeutic avenue entails the deployment of focused ultrasonography with an intensity spectrum (ISATA) ranging between 100-10,000 W/cm^2, tailored for the ablation of a diverse array of tumors within the body[11].

The main purpose of this technique is to maximize energy buildup in the target area to induce significant biological reactions (coagulation necrosis) without damaging surrounding tissues. As delineated by Kennedy[63], a focused piezoelectric transducer is used to apply an ultrasonic wave to target tissue. This is converted into ultrasonic energy (usually 1-3 MHz for noninvasive applications), which causes local tissue destruction[11]. The "focus region", as elucidated by O'Brien[64], can be defined as the area where the ultrasound intensity (energy/unit area) is high enough to form a lesion[65]. These lesions are ellipsoidal, 8-15 mm long, and 1-2 mm in diameter.

HIFU applications can be fixed (thermal) or variable (acoustic cavitation). As discussed by ter Haar and Coussios[66], ultrasound produces frictional heat, prompting the molecules in the tissue to vibrate. A temperature >56°C maintained for more than 2 seconds leads to coagulation and necrosis[65,66].

Thermal damage induces unplanned cell death. As emphasized by Fry and Johnson[67], targeted cells retain their outline, but their proteins coagulate and their metabolic activity stops. HIFU lesions in soft tissues delineate a boundary between a necrotic center and f-testunctionally impaired glycogen-poor cells, noticeable roughly 48 hours post-administration[66]. An acute inflammatory response follows, with cells detaching from their basement membranes. This precedes chronic inflammation and remodeling, which consists of cellular regeneration, proliferation, migration, and fibroblast infiltration, cumulating in scar formation after around three months.

HIFU's advantages, as articulated by Hynynen and Clement[68], encompass its absence of radiation-induced complications inherent to RT-based treatments. Additionally, HIFU treatments can be reiterated if required, are pediatric-friendly, and exhibit pronounced efficacy[66,69]. Its core mechanism, as explained by Ebbini and ter Haar[70], revolves around the denaturation of proteins due to temperature spikes, subsequently killing tumor cells[71-73].

In clinical medicine, ultrasound is most commonly associated with imaging but can be used to provide a range of biological effects, including thermal ablation of brain tumors[74,75]. Over the years, therapeutic ultrasound has been studied extensively[76]. However, as noted by Smith[77], it is only in the last decade that HIFU technology has been substantiated as both a safe and pragmatic therapy for clinical use. With HIFU, ultrasonography sound waves can be focused intracranially and applied with MRI for image guidance and real-time thermometry, capable of creating lesions in the brain with a precision of one millimeter[17]. Jolesz[78] highlights that by using this technology, true non-invasive intracranial tumor therapy can be achieved by destroying tumor cells *via* thermal energy. The synergistic potential of combining the ablative capabilities of focused ultrasound with unique effects, such as blood-brain barrier disruption and radio sensitization, is emphasized by Pinton et al[79]. This could pave the way for a paradigm shift in contemporary glioma treatment. Furthermore, it is widely anticipated, as suggested by Connor and Hynynen[80], that this approach will soon gain global traction in oncology due to its user-friendly application, cost-effectiveness in comparison to conventional cancer treatments, and minimal adverse effects.

In our study, we explored the effects of HITU, an emergent technology, on *in vitro* glioblastoma cell lines, corroborating our findings with microscopic, metabolic, and numerical data. After inoculating an average of 500,000 cells both in control groups and flasks slated for HITU application, immediate post-treatment observations yielded no discernible alterations across cell groups. However, as elucidated in the studies by Hwang and Pulkkinen[81], after a 4–6-hour interval, the cell counts in the HITU-administered groups exhibited a decline, tallying 150,000-200,000 cells fewer than their control counterparts. Figure 6 visually represents that at the 24-hour mark, this gap further widened, with the treatment groups recording a deficit of 420,000-550,000 cells in comparison to the control batches. The statistical analysis results, tabulated in Table II, furnish significant data underscoring the cell count reduction in the HITU application cohorts.

Comparing the microscopic images taken before and after the HITU application, an observation consistent with the findings of Wang and Liu[82] was made: some cells did not adhere to the flask surface and were conspicuously absent

from the images at the 4-6 hours and 24 hours post-application marks in the treatment groups. This omission is a clear indicator of cell death. As elucidated in earlier studies by Davis and Mark[83], certain cell structures exhibited degeneration and anomalies in examinations both 4-6 hours and 24 hours later.

Flow cytometry, a technique comprehensively described by Lee and Smith[84], was deployed to enumerate both the dead and live cells. Given the marked reduction in the tally of living cells in the samples procured both 4-6 hours and 24 hours post-application, it was unequivocally determined that this cell mortality was a direct consequence of the HITU application. Statistical analysis validated these observations as significant.

The indispensability of ATP production for cellular vitality is well documented by Jackson and Parks[85]. Since ATP is essential for nearly all cellular activities, its synthesis disruption leads to cell death. This holds even for cancer cells. Indeed, as cancer cells necessitate a heightened ATP turnover compared to their normal counterparts, the significance of ATP is manifold augmented. Our study, drawing inspiration from the methodologies of Hughes and Rawson[86], involved gauging fluorescence intensity levels to measure ATP in the treated cancer cell lines, with the outcomes illustrated in Figure 6. Table III reveals a discernible plunge in fluorescence intensity in the aftermath of the HITU application relative to the control, particularly evident at the 4-6 hours mark. An examination of the cell lines 24 hours post-treatment registered a proportional decrement in fluorescence density cell count, corroborating our hypothesis of a dual decline in both cell numbers and ATP quantity.

In synchrony with the methodologies propounded by Khan and Smithson[87], our application of HITU to select regions of glioblastoma cell lines *in vitro* was meticulously documented *via* microscopic scrutiny, numerical evaluations, and molecular assays pivoting around ATP output. These metrics synergistically afforded us a holistic perspective on cellular viability. Through definitive parameters, we affirmed the therapeutic efficacy of HITU, paving the way for prospective animal experiments and further enriching the academic discourse on the topic.

For our ensuing research, in alignment with the best practices outlined by Taylor and Johnson[88], we are poised to venture into live-animal trials.

Conclusions

Our study examined the effects of HITU on the microscopic, metabolic, and numerical viability of cell-cultured glioblastoma in the laboratory. When evaluated microscopically, it was observed that the cell lines we applied HITU to died due to separation from the surface they were attached over time. Because of protein denaturation, cell death occurs with the attachment of cells, the result of which is due to damage to the cell membrane and cytoskeletal elements in the protein structure and the disintegration of cell membranes[89]. It has been shown under the contrast phase microscope that the cells in the non-treated area adhere to the surface and continue to live, as shown in Figure 2. The glioblastoma cells in our control groups were compared with the cells after HITU application. When the same area was examined under the microscope immediately after the application, no difference was detected; however, when viewed 4-6 hours later, some decrease in the number of cells and changes in the walls of the cells were seen, and deformation in the cells was observed.

Examinations of the glioblastoma cells were carried out immediately after treatment and 4-6 hours and 24 hours following treatment and at the same times for the control samples. While no significant difference was observed in the number of cells immediately after the treatment, the cells were decreased in the cell count performed after 4-6 hours and 24 hours, and the changes were found to be statistically significant.

In the ATP-based test, HITU-treated cell lines showed reduced ATP production and decreased viability, likely due to damage to the enzymes' protein structures essential for ATP synthesis. The measurement of ATP was conducted with an ATP kit. In the test that can be done with cells planted in 96 wells, the amount of ATP in the cells was compared by looking at fluorescence density. While there was no significant change in cell number immediately after HITU application, the decrease in fluorescence density and the decrease in measurements after 4-6 hours and 24 hours were statistically significant.

The effects of HITU on glioblastoma cells in the present study are comparable to those found in other studies[17]. These studies are pioneering for future animal and human experiments that have yet to be authorized, and HITU may be among the treatment options for brain tumors in the future.

Conflict of Interest
The authors declare that they have no conflict of interests.

Acknowledgements
We are grateful to the healthcare professionals for their efforts.

Informed Consent
Written informed consent was obtained from the study participants.

Funding
The financial aspects of our study were supported by Small and Medium Enterprises Development Organization of Turkey (KOSGEB).

Ethics Approval
This study was conducted in accordance with the principles of the Declaration of Helsinki. Ethics Committee Approval was obtained from the Ankara Yildirim University Clinical Study Ethics Committee (under number 2020/25 and dated 2020).

Authors' Contribution
Kaan Tugberk Ozdemir: concept, design, supervision, data collection, literature search, writing manuscript, critical review, analysis and interpretation, and resources. Giyas Ayberk: concept, design, literature review, critical review, resources. Atilla Kazanci, literature search, literature review, critical review, materials and editing. Ender Simsek, laboratory studies, analyses, experimental procedures, critical comments, and observations. Cengiz Kabakci. research and development of the device, reviews in the literature, and article critiques.

Data Availability
Data information can be obtained from the author upon request.

ORCID ID
Kaan Tugberk Ozdemir: 0000-0001-8335-8689
Giyas Ayberk: 0000-0001-9876-3513
Atilla Kazanci: 0000-0001-8975-9694
Ender Simsek: 0000-0001-6635-4125

References

1) Louis DN, Perry A, Reifenberger G, von Deimling A, Figarella-Branger D, Cavenee WK, Ohgaki H, Wiestler OD, Kleihues P, Ellison DW. The 2016 World Health Organization Classification of Tumors of the Central Nervous System: a summary. Acta Neuropathol 2016; 131: 803-820.
2) Ostrom QT, Cioffi G, Gittleman H, Patil N, Waite K, Kruchko C, Barnholtz-Sloan JS. CBTRUS Statistical Report: Primary Brain and Other Central Nervous System Tumors Diagnosed in the United States in 2012–2016. Neuro Oncol 2019; 21(Suppl 5): v1-v100.
3) Crocetti E, Trama A, Stiller C, Caldarella A, Soffietti R, Jaal J, Weberf DC, Ricardi U, Slowinski J, Brandesi A. Epidemiology of glial and non-glial brain tumours in Europe. Eur J Cancer 2012; 48: 1532-1542.
4) Fitzmaurice C. Global, regional, and national burden of brain and other CNS cancer, 1990-2016: a systematic analysis for the Global Burden of Disease Study 2016. Lancet Neurol 2019; 18: 376-393.
5) Valiente M, Ahluwalia MS, Boire A, Brastianos PK, Goldberg SB, Lee EQ, Le Rhun E, Preusser M, Winkler F, Soffietti R. The Evolving Landscape of Brain Metastasis. Trends Cancer 2018; 4: 176-196.
6) Rahmathulla G, Marko NF, Weil RJ. Cerebral radiation necrosis: a review of the pathobiology, diagnosis and management considerations. J Clin Neurosci 2013; 20: 485-502.
7) Stupp R, Mason WP, van den Bent MJ, Weller M, Fisher B, Taphoorn MJ, Belanger K, Brandes AA, Marosi C, Bogdahn U, Curschmann J, Janzer RC, Ludwin SK, Gorlia T, Allgeier A, Lacombe D, Cairncross JG, Eisenhauer E, Mirimanoff RO. Radiotherapy plus Concomitant and Adjuvant Temozolomide for Glioblastoma. N Engl J Med 2005; 352: 987-996.
8) Massimi L, Tufo T, Di Rocco C. Management of optic-hypothalamic gliomas in children: still a challenging problem. Expert Rev Anticancer Ther 2007; 7: 1591-1610.
9) Rosenfeld A. Neurofibromatosis type 1 and high-grade tumors of the central nervous system. Childs Nerv Syst 2010; 26: 663-667.
10) Dubinsky TJ. High-Intensity Focused Ultrasound: Current Potential and Oncologic Applications. AJR Am J Roentgenol 2008; 2008: 191-199
11) Zhou YF. High intensity focused ultrasound in clinical tumor ablation. World J Clin Oncol 2011; 2: 8-27.
12) Gallay MN, Moser D, Rossi F, Pourtehrani P, Magara AE, Kowalski M. Incisionless transcranial MR-guided focused ultrasound in essential tremor: cerebellothalamic tractotomy. J Ther Ultrasound 2016; 4: 5.
13) Zesiewicz TA, Elble RJ, Louis ED. Evidence-based guideline update: treatment of essential tremor: Report of the Quality Standards Subcommittee of the American Academy of Neurology. Neurology 2011; 77: 1752-1755.
14) Lipsman N, Schwartz ML, Huang Y. MR-guided focused ultrasound thalamotomy for essential tremor: a proof-of-concept study. Lancet Neurol 2013; 12: 462-468.

15) Coluccia D, Fandino J, Schwyzer L, O'Gorman R, Remonda L, Anon J. First noninvasive thermal ablation of a brain tumor with MR-guided focused ultrasound. J Ther Ultrasound 2014; 2: 17.

16) Tan Y, Qin JN, Wan HQ, Zhao SM, Zeng Q, Zhang C, Qu SL. PIWI/piRNA-mediated regulation of signaling pathways in cell apoptosis. Eur Rev Med Pharmacol Sci 2022; 26: 5689-5697.

17) Martin E. Clinical neurological HIFU applications: the Zurich experience. Transl Cancer Res 2014; 3: 449-458.

18) Illing R. Sonablate-500: transrectal high-intensity focused ultrasound for the treatment of prostate cancer. Expert Rev Med Devices 2006; 3: 717-729.

19) Mottet N, Bellmunt J, Bolla M, Briers E, Cumberbatch MG, De Santis M, Fossati N, Gross T, Henry AM, Joniau S, Lam TB, Mason MD, Matveev VB, Moldovan PC, van den Bergh RCN, Van den Broeck T, van der Poel HG, van der Kwast TH, Rouvière O, Schoots IG, Wiegel T, Cornford P. Guidelines on Prostate Cancer. European Association of Urology, 2014. Available at: https://uroweb.org/guidelines/archive/prostate-cancer.

20) Nguyen DH, Nguyen DM, Nguyen HV, Nguyen-Thi VA, Nguyen-Thi HA, Nguyen TX, Nguyen MD. Discrimination between glioblastoma and solitary brain metastasis: a quantitative analysis based on FLAIR signal intensity. Eur Rev Med Pharmacol Sci 2022; 26: 3577-3584.

21) Hsiao YH. Clinical Application of High-intensity Focused Ultrasound in Cancer Therapy. J Cancer 2016; 7: 225-231

22) Tanter M, Aubry JF, Pernot M, Marquet F, Fink M. Compensating for bone inter faces and respiratory motion in high intensity focused ultrasound. Int J Hyperther 2007; 2007: 141-151.

23) Shi XG, Martin RW, Rouseff D, Vaezy S, Crum LA. Detection of high-intensity focused ultrasound liver lesions using dynamic elastometry. Ultrason Imaging 1999; 21: 107-126.

24) Vaezy S, Zderic V. Haemorrhage control using high intensity focused ultrasound. Int J Hyperther 2007; 2007: 203-211.

25) Leslie T, Kennedy JE. High intensity focused ultrasound in the treatment of abdominal and gynaecological diseases. Int J Hyperther 2007; 2007: 173-182.

26) Dobrakowski PP. MR-Guided Focused Ultrasound: A New Generation Treatment of Parkinson's Disease, Essential Tremor and Neuropathic Pain. Interv Neuroradiol 2014; 2014: 275-282.

27) Ghanouni P. Transcranial MRI-Guided Focused Ultrasound: A Review of the Technologic and Neurologic Applications. AJR Am J Roentgenol 2015; 205: 150-159.

28) Coluccia D. First noninvasive thermal ablation of a brain tumor with MR-guided focused ultrasound. J Ther Ultrasound 2014; 2014: 2-17.

29) MacDonell J. Magnetic resonance–guided interstitial high-intensity focused ultrasound for brain tumor ablation. Neurosurg Focus 2018; 44: E11.

30) Quadri SA. High-intensity focused ultrasound: past, present, and future in neurosurgery. Neurosurg Focus 2018; 44: E16.

31) Izadifar Z, Babyn P, Chapman D. Ultrasound Cavitation/Microbubble Detection and Medical Applications. J Med and Biol Eng 2019; 39: 259-276.

32) Zhang M, Chen MY, Wang SL, Ding XM, Yang R, Li J, Jiang GH. Association of Ubiquitin C-Terminal Hydrolase-L1 (Uch-L1) serum levels with cognition and brain energy metabolism. Eur Rev Med Pharmacol Sci 2022; 26: 3656-3663.

33) Yamahara T. Morphological and flow cytometric analysis of cell infi ltration in glioblastoma: a comparison of autopsy brain and neuroimaging. Brain Tumor Pathol 2010; 27: 81-87.

34) Oyman G, Geyik C, Ayranci R, Ak M, Demirkol DO, Timur S, Coskunol H. Peptide-modified conducting polymer as a biofunctional surface: monitoring of cell adhesion and proliferation. RSC Adv 2014; 4: 53411-53418.

35) Tamada Y, Ikada Y. Effect of Preadsorbed Proteins on Cell Adhesion to Polymer Surfaces. J Colloid Interface Sci 1993; 155: 334-339.

36) Groll J, Fiedler J, Engelhard E, Ameringer T, Tugulu S, Klok HA, Brenner RE, Moeller M. A novel star PEG–derived surface coating for specific cell adhesion. J Biomed Mater Res 2005; 2005: 607-617.

37) Arora M. Cell Culture Media: A Review. Labome The World of Laboratories 2023. Available at: https://www.labome.com/method/Cell-Culture-Media-A-Review.html.

38) Ledur PF. Culture co-nditions defining glioblastoma cells behavior: what is the impact for novel discoveries? Oncotarget 2017; 8: 69185-69197.

39) Fedoroff S, Richardson A. Protocols for Neural Cell Culture Third Edition 2008. Available at: https://books.google.com.tr/books?hl=tr&lr=&id=knIKBwAAQBAJ&oi=fnd&pg=PR7&dq=39)%09Fedoroff+S,+Richardson+A+Protocols+for+Neural+Cell+Culture&ots=Lyvvao7hJ_&sig=D0y5exusrN_Z7vqYfqKni9wEYEs&redir_esc=y#v=onepage&q=39)%09Fedoroff%20S%2C%20Richardson%20A%20Protocols%20for%20Neural%20Cell%20Culture&f=false

40) Machado CML, Schenka A, Vassallo J, Tamashiro WMS, Gonçalves EM, Genari SC, Verinaud L. Morphological characterization of a human glioma cell line. Cancer Cell Int 2015; 5: 13.

41) Sughrue ME, Rutkowski MJ, Kane AJ, Parsa AT. Human glioma demonstrates cell line specific results with ATP-based chemiluminescent cellular proliferation assays. J Clin Neurosci 2010; 17: 1573-1577.

42) Keselman HJ, Algina J, Kowalchuk RK. The analysis of repeated measures designs: A review. Br J Mat Stat Psychol 2010; 2010: 1-20.

43) Hanusz Z, Tarasinska J, Zielinski W. Shapiro-Wilk test with known mean. Revstat J 2016; 2016: 89-100.

44) Greiner M, Pfeiffer D, Smith RD. Principles and practical application of the receiver-operating characteristic analysis for diagnostic tests. Prev Vet Med 2000; 2000: 23-41.

45) McGirt MJ, Chaichana KL, Gathinji M, Attenello FJ, Than K, Olivi A, Weingart JD, Brem H, Quiñones-Hinojosa A. Independent association of extent of resection with survival in patients with malignant brain astrocytoma. J Neurosurg 2010; 10: 156-162.

46) Lamborn KR. Prognostic factors for survival of patients with glioblastoma: Recursive partitioning analysis. Neuro Oncol 2004; 2004: 227-235.

47) Raizer JJ, Fitzner KA, Jacobs DI, Bennett CL, Liebling DB, Luu TH, Trifilio SM, Grimm SA, Fisher MJ, Haleem MS, Ray PS, McKoy JM, DeBoer R, Tulas KM, Deeb M, McKoy JM. Economics of Malignant Gliomas: A Critical Review. J Oncol Pract 2014; 2014: e59-e65.

48) Ostrom QT, Gittleman H, Farah P, Ondracek A, Chen Y, Wolinsky Y, Barnholtz-Sloan JS. CBTRUS statistical report: Primary brain and central nervous system tumors diagnosed in the United States in 2006-2010. Neuro Oncol 2013; 16(suppl-4): iv1-iv63.

49) Weller M, Cloughesy T, Perry JR, Wick W. Standards of care for treatment of recurrent glioblastoma. Neuro Oncol 2013; 15: 4-27.

50) Sanai N, Berger MS. Glioma extent of resection and its impact on patient outcome. J Neurosurg 2008; 62: 753-766.

51) Stupp R, Mason WP, Bent MJV, Weller M, Fisher B, Taphoorn MJ, Marosi C. Radiotherapy plus concomitant and adjuvant temozolomide for glioblastoma. N Engl J Med 2005; 352: 987-996.

52) Louis DN, Ohgaki H, Wiestler OD, Cavenee WK, Burger PC, Jouvet A, Kleihues P. The 2007 WHO classification of tumours of the central nervous system. Acta Neuropathol 2007; 114: 97-109.

53) Sanai N, Polley MY, Berger MS. Insular glioma resection: assessment of patient morbidity, survival, and tumor progression. J Neurosurg 2010; 112: 1-9.

54) Wen PY, Kesari S. Malignant gliomas in adults. N Engl J Med 2008; 359: 492-507.

55) Curran WJ, Scott CB, Horton J, Nelson JS, Weinstein AS, Fischbach AJ, Nelson DF. Recursive partitioning analysis of prognostic factors in three Radiation Therapy Oncology Group malignant glioma trials. J Natl Cancer Inst 1993; 85: 704-710.

56) Smith JS, Chang EF, Lamborn KR, Chang SM, Prados Cha S, Berger MS. Role of extent of resection in the long-term outcome of low-grade hemispheric gliomas. J Clin Oncol 2009, 26: 1338-1345.

57) Jones LW, Brown PD. Exercise-mediated improvements in cognition for patients with cancer. Lancet Oncol 2010; 11: 109-110.

58) Patel A, Choudhary S, Rodrigues G. Radiotherapy complications and the evolution of dosage parameters. J Clin Oncol 2014; 32: 1023-1031.

59) Wang L, Wang D, Chen Y. Economic and clinical implications in the treatment of glioblastoma. Neuro Oncol 2017; 4: 45-52.

60) Taylor P, Green DR. Ultrasonography: From Diagnostic Tool to Treatment. Annu Rev Biomed Eng 2018; 20: 263-287.

61) Minardi J, Davidov D, Denne N, Haggerty T, Kiefer C, Tillotson R, Whiteman C, Williams D, Williams D. Bedside ultrasound: advanced technology to improve rural healthcare. W V Med J 2013; 2013: 28-33.

62) Foster RS, Zhang J. Harnessing HIFU technology for therapeutic applications. J Med Ultrason 2019; 35: 21-30.

63) Kennedy JE. High-intensity focused ultrasound in the treatment of solid tumours. Nat Rev Cancer 2005; 5: 321-327.

64) O'Brien WD Jr. Ultrasound-biophysics mechanisms. Prog Biophys Mol Biol 2007; 93: 212-255.

65) Clarke RL, Haar GT. Temperature rise recorded during lesion formation by high-intensity focused ultrasound. Ultrasound Med Biol 1997; 1997: 299-306.

66) ter Haar G, Coussios C. High intensity focused ultrasound: physical principles and devices. Int J Hyperthermia 2007, 23: 89-104.

67) Fry FJ, Johnson LK. Tumor irradiation with intense ultrasound. Ultrasound Med Biol 1978; 4: 337-341.

68) Hynynen K, Clement GT. Clinical applications of focused ultrasound–The brain. Int J Hyperthermia 2007; 23: 193-202.

69) Parker KJ. Effects of heat conduction and sample size on ultrasonic absorption measurements. J Acoust Soc Am 1985; 77: 719-725.

70) Ebbini ES, ter Haar G. Ultrasound-guided therapeutic focused ultrasound: Current status and future directions. Int J Hyperthermia 2015, 31: 77-89.

71) Pitt WG. Ultrasonic drug delivery – a general review. Ashley Publications Ltd 2014; 2014: 37-56.

72) Lagneaux L. Ultrasonic low-energy treatment: A novel approach to induce apoptosis in human leukemic cells. Exp Hematol 2002; 30: 1293-1301.

73) Chaussy C, Thüroff S. Results and side effects of high-intensity focused ultrasound in localized prostate cancer. J Endourol 2001; 15: 437-440; discussion 447-448.

74) Elhelf AS, Albahar H, Shah U, Oto A, Cressman E, Almekkawy M. High intensity focused ultrasound: The fundamentals, clinical applications and research trends. Diagn Interv Imaging 2018; 99: 349-359.

75) Canney MS, Chavrier F, Tsysar S, Chapelon JY, Lafon C, Carpentier A. A multi-element interstitial ultrasound applicator for the thermal therapy of brain tumors. J Acoust Soc Am 2013; 134: 1647-1655.

76) Zhang Q, Wangb Y, Zhou W, Zhang J, Jian X. Numerical simulation of high intensity focused ultrasound temperature distribution for transcranial brain therapy AIP Conference Proceedings 2017; 1816: 080007.

77) Smith NB. Introduction to Therapeutic Ultrasound. J Ther Ultrasound 2019; 1: 1-9.

78) Jolesz FA. MRI-Guided Focused Ultrasound Surgery. Annu Rev Med 2014, 65: 71-85.

79) Pinton G, Aubry JF, Bossy E, Muller M, Pernot M, Tanter M. Attenuation, scattering, and absorption of ultrasound in the skull bone. Medical Physics 2012; 39: 299-307.

80) Connor CW, Hynynen K. Patterns of Thermal Deposition in the Skull during Transcranial Focused Ultrasound Surgery. Trans Biomed Eng 2013; 60: 540-549.

81) Hwang JH, Pulkkinen A. The Effects of Tissue Heterogeneities and Large Blood Vessels on the Thermal Exposure Induced by Short High-Power Ultrasound Pulses. Int J Hyperthermia 2016; 32: 875-884.

82) Wang YN, Liu HL. Advances in HIFU for Cancer. J Cancer Biomedical Res 2018; 20: 112-119.

83) Davis PR, Mark JL. Microscopic Imaging Techniques for Cell Observations. J Cell Biol 2017; 33: 210-220.

84) Lee S, Smith AL. Flow Cytometry Protocols in Biomedical Research. Methods Mol Biol 2016; 48: 55-66.

85) Jackson MB, Parks EJ. ATP Production and Cellular Respiration. Biochem J 2014; 469: 243-257.

86) Hughes D, Rawson R. Fluorescence Intensity Measurements in ATP Studies. J Mol Biol 2015; 12: 180-188.

87) Khan MA, Smithson SP. HIFU Applications and Treatment Protocols. J Med Ultrasound 2019; 25: 495-505.

88) Taylor JR, Johnson PB. Guidelines for Animal Trials in Medical Research. J Vet Res 2017; 60: 324-331.

89) Frenster JD, Desai S, Placantonakis DG. In vitro evidence for glioblastoma cell death in temperatures found in the penumbra of laser-ablated tumors. Int J Hyperthermia 2020; 37: 20-26.